

## Isothermal Annealing below 60°K of Deuteron Irradiated Noble Metals\*

G. D. MAGNUSON,† W. PALMER, AND J. S. KOEHLER  
*University of Illinois, Urbana, Illinois*

(Received November 8, 1957)

Foils of 99.999% pure copper, 99.999% pure silver, and a copper alloy containing 3.78 atomic percent nickel were irradiated near liquid helium temperature with 10.7-Mev deuterons. Annealing up to 60°K was performed in a series of isothermal steps. During each anneal the decrease of the radiation-induced resistivity increment with time was observed. Resistivity distribution curves, obtained by assuming that recovery processes with a continuum of activation energies are present, show several small peaks followed by a large peak. The maxima occur at 0.048, 0.080, 0.091, and 0.113 ev in copper and at 0.045, 0.058, and 0.079 ev in silver. The frequency factors for both metals were found to lie between  $7.2 \times 10^{10}$  and  $3.9 \times 10^{12}$  sec<sup>-1</sup>. Alloying served to broaden the energy distribution of the recovery processes. Changes in the Debye characteristic temperature of  $-(15 \pm 1)^\circ\text{K}$  and  $-(10 \pm 1)^\circ\text{K}$  were also observed in copper and silver, respectively. Annealing of these changes was about 80% complete at 50°K. The dominant mechanism in the low-temperature recovery is believed to be the annihilation of Frenkel pairs, with the interstitials as the mobile defects. A trapping model is proposed to explain why all the resistivity increment does not anneal out once interstitials begin to move.

### I. INTRODUCTION

DURING the last few years there have been a number of experiments designed to determine the nature of the low-temperature annealing which occurs in irradiated noble metals.<sup>1</sup> It is observed that if copper and silver are irradiated at about 10°K with 1-Mev neutrons,<sup>2</sup> 10-Mev deuterons,<sup>3</sup> or 1-Mev electrons,<sup>4</sup> an appreciable annealing of the resistivity increment occurs at about 30°K. Recent work at the University of Illinois shows that the length<sup>5</sup> and lattice parameter<sup>6</sup> increments anneal out in about the same way as the resistivity increment. Blewitt and co-workers<sup>7</sup> find an anomalously small amount of energy released in pile irradiated specimens in this temperature range. At temperatures somewhat above 40°K the above observations reveal a continuum of annealing processes such that each increase in temperature produces a small amount of recovery.

Lomer and Cottrell<sup>8</sup> have proposed that small impurity atoms can trap the interstitial configuration, and Blewitt and co-workers<sup>9</sup> have shown that 0.1% of Be,

Si, and Au in copper can appreciably influence the annealing. They have also found<sup>9</sup> that the annealing of irradiated copper is not influenced by cold work or by altering the amount of irradiation by a factor of 50.

The present research was undertaken to ascertain whether or not gold shows the low-temperature drop, to determine the frequency factor and the spectrum of activation energies on specimens of high purity, to discover whether the annealing is significantly altered if the purity is increased by an order of magnitude, and to determine the effect of irradiation on the Debye  $\Theta$ .

### II. EXPERIMENTAL

#### 1. Method and Apparatus

Resistance *versus* temperature curves of the unbombarded specimens, as well as thermocouple calibrations, were obtained in the laboratory before mounting the cryostat on the cyclotron. During irradiation the cryostat was separated from the cyclotron chamber by a 0.025-mm Duraluminum diaphragm. This served to eliminate the adsorption of deuterium and other gases on the low-temperature parts of the apparatus. In previous experiments<sup>3</sup> evolution of these adsorbed gases caused a rapid rise in temperature during annealing following irradiation. No such temperature pulse occurred in this experiment.

During irradiation and subsequent annealing, a high-vacuum system maintained a pressure less than  $5.0 \times 10^{-6}$  mm of Hg as determined by a Phillips ionization gauge mounted on the outer cryostat wall. The deuteron flux was measured by insulating the inner part of the cryostat from ground by a Teflon gasket and passing the charge collected through an electronic current integrator.<sup>10</sup> Alignment of the foils in the cyclotron beam was accomplished by mounting the cryostat on an adjustable stand and maximizing the beam current

\* This work was partially supported by the U. S. Atomic Energy Commission.

† Now at Convair, Physics Section, San Diego, California.

<sup>1</sup> For a recent review see F. Seitz and J. S. Koehler, in *Solid State Physics*, edited by F. Seitz and D. Turnbull (Academic Press, Inc., New York, 1956), Vol. 2, p. 305. For other reviews see J. W. Glen, in *Advances in Physics*, edited by N. F. Mott (Taylor and Francis, Ltd., London, 1955), Vol. 4, p. 381; G. H. Kinchin and R. S. Pease, in *Reports on Progress in Physics* (The Physical Society, London, 1955), Vol. 18, p. 1; H. Brooks, in *Annual Review of Nuclear Science* (Annual Reviews, Inc., Stanford, 1956), Vol. 6, p. 215.

<sup>2</sup> Redman, Noggle, Coltman, and Blewitt, *Bull. Am. Phys. Soc. Ser. II*, **1**, 130 (1956).

<sup>3</sup> Cooper, Koehler, and Marx, *Phys. Rev.* **97**, 599 (1955).

<sup>4</sup> Corbett, Denney, Fiske, and Walker, *Phys. Rev.* **104**, 851 (1956).

<sup>5</sup> R. W. Vook and C. A. Wert, *Phys. Rev.* **109**, 1529 (1958).

<sup>6</sup> R. O. Simmons and R. W. Balluffi, *Phys. Rev.* **109**, 335 (1958).

<sup>7</sup> Blewitt, Coltman, Noggle, and Holmes, *Bull. Am. Phys. Soc. Ser. II*, **1**, 130 (1956).

<sup>8</sup> W. M. Lomer and A. H. Cottrell, *Phil. Mag.* **46**, 711 (1955).

<sup>9</sup> Blewitt, Coltman, Klabunde, and Noggle, *J. Appl. Phys.* **28**, 639 (1957).

<sup>10</sup> A modified version of a device described by H. T. Gittings, Jr., *Rev. Sci. Instr.* **20**, 325 (1949).

received. During bombardment the Cu and Ag foils were maintained at a temperature no greater than 10.8°K, and the CuNi foil was kept below 21.1°K.

The isothermal annealing data after irradiation were taken without removing the cryostat from the cyclotron. Resistance measurements were made using standard potentiometric methods. A Rubicon thermofree Cat. No. 2767 microvolt potentiometer with a Rubicon Cat. No. 3550 photoelectric galvanometer was used to measure the voltage across the foils. The measuring current for the Cu and Ag foils was 0.1 amp and was constant to 1 part in 50 000. The measuring current for the CuNi foil was 0.02 amp and was constant to 1 part in 40 000.

Instrumental error in a single measurement of the resistance of the Cu and Ag foils was  $\pm 0.1 \times 10^{-6}$  ohm. The corresponding error for the CuNi foil was  $\pm 1 \times 10^{-6}$  ohm. These values are 0.11, 0.070, and 0.36% of the maximum observed resistance increment in Cu, Ag, and CuNi, respectively. To eliminate the effect of stray thermal voltages in the potential leads, the direction of the current was reversed and the average of the two voltage readings was used.

The cryostat used in this research was of the same design as that used by Cooper<sup>3</sup> and is described more fully elsewhere.<sup>11</sup> However, it was modified by the insertion of a "heat switch" between the copper specimen mounting block and the liquid helium sphere. This heat switch allowed one to hold the foils at any temperature from 7 to 78°K without an excessive expenditure of liquid helium.<sup>12</sup> This device is shown in cross section in Fig. 1. The tube for evacuation of the heat switch runs up to the cover plate of the cryostat. To increase the pumping speed of the system  $\frac{1}{4}$  in. holes were drilled at the top and bottom of the copper cylinders. For clarity these holes are not shown in Fig. 1.

When the heat switch was evacuated ( $10^{-5}$  mm of Hg), the only conduction path between the block and the liquid helium sphere was through the stainless steel cylinder, radiation transfer between adjacent cylinders being negligible. In this condition it functioned to thermally isolate the block and foils from the liquid helium, thus permitting the temperature of the block to be raised without an excessive consumption of liquid helium. When the device was filled with helium gas to a pressure of about 0.1 mm of Hg, heat conduction between adjacent cylinders became appreciable and maximum cooling of the block was obtained. It was found that the thermal conductivity of the heat switch in its filled condition was about 70 times its conductivity while evacuated.

To raise the temperature of the block and foils, a small 60-ohm heater was attached to the block. Since it was necessary to make temperature changes as quickly

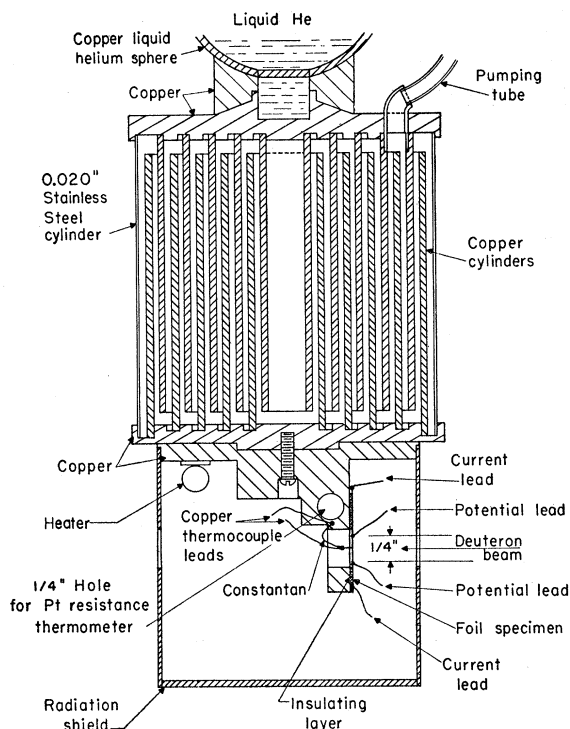


Fig. 1. Cross section of heat switch and mounting block showing details of thermocouple construction and placement of the foil current and potential leads.

as possible, a key was incorporated in the heater circuit so that large current pulses could be sent through the heater. When the desired temperature was reached, a small current of the order of 5–100 ma maintained the temperature constant. By careful manipulation of the heater current the temperature of the block could be maintained constant to  $\pm 0.02^\circ\text{K}$ . The time required to raise the temperature  $1.5^\circ\text{K}$  was about 20 sec at  $20^\circ\text{K}$  and about 40 sec in the  $40^\circ\text{K}$  region.

## 2. Specimen Preparation and Mounting

The specimens used in this research were in the form of polycrystalline foils. The primary reason for using foils rather than wires was the relative ease with which foils of the requisite purity could be fabricated. To obtain a qualitative test of the purity, the resistivity of the mounted specimen at  $0^\circ\text{C}$  was compared with that at  $4.2^\circ\text{K}$ . The ratio  $\rho_{0^\circ\text{C}}/\rho_{4.2^\circ\text{K}}$  was 1110 for Cu, 798 for Ag, and 770 for Au.

The copper was American Smelting and Refining Company's continuously-cast, high-purity  $\frac{3}{8}$ -in. diameter rod.<sup>13</sup> This material had a residual resistivity of less than  $1.3 \times 10^{-9}$  ohm-cm and a stated purity of about 99.999%. The rod was rolled to a 0.004-in. foil from which 0.5-mm wide specimens were cut.

The CuNi alloy was prepared by Horizons, Inc. in

<sup>11</sup> D. E. Mapother and F. E. L. Witt, Rev. Sci. Instr. 26, 843 (1955).

<sup>12</sup> We are indebted to D. E. Mapother for suggestion of the method and to F. E. L. Witt for construction of the device.

<sup>13</sup> Smart, Smith, and Phillips, Trans. Am. Inst. Mining Met. Engrs. 143, 272 (1941).

the form of a  $\frac{3}{8}$ -in. diameter rod and was ascertained by an independent testing laboratory to consist of 3.78 at % Ni. Specimens 0.5 mm wide were cut from the foil obtained by rolling the rod to a thickness of 0.0025 in.

The Ag was Johnson Matthey 99.999% pure 1.2-mm diameter rod, catalog No. J. M. 52. This was rolled to a 0.0035-in. foil from which 0.5-mm wide specimens were cut.

The Au was obtained from Sigmund Cohn Company in the form of 99.999% pure 0.030-in. wire. This was rolled to a 0.004-in. foil from which 0.5-mm wide foils were cut.

After cutting, the foils were cleaned and etched to remove any surface oxides and then annealed in a high vacuum (less than  $3.0 \times 10^{-5}$  mm of Hg) furnace at 600°C for one hour. After annealing, 0.004-in. copper current and potential leads were carefully soldered to the specimens, which were then mounted on the copper specimen block as shown in Fig. 1.

It was imperative that the foils be mounted in such a manner that good thermal contact with the block was obtained and at the same time be electrically insulated from the block. To accomplish both these ends the following method was used. A very thin coating of Duco cement was first applied to the front face of the block and allowed to dry. The foil was then glued in place with an aqueous solution of polyvinyl alcohol, the use of which was prompted by the fact that it would not disturb the insulating layer of Duco. This method satisfied both requirements and permitted easy mounting of the foils with the introduction of negligible cold work.

After the specimens were mounted, the current and potential leads were insulated with Fiberglas sleeving and clamped to the block with copper bars for the twofold purpose of preventing undue strain of the solder joints and reducing heat conduction to the foils.

The block was attached to the bottom of the heat switch with a 5–40 screw and a thin layer of G.E. 7031 varnish. To aid in achieving a uniform temperature distribution the foils were enclosed in a copper radiation shield as shown in Fig. 1. The rectangular hole in the mounting block and the apertures in the block radiation shield permitted the deuteron beam to pass through without dissipating its entire energy in parts cooled by liquid helium. The beam impinged instead on an outer radiation shield which was cooled by liquid nitrogen and surrounded the entire block assembly. 0.5-mil Cu foils placed over the apertures of both radiation shields were used to complete the thermal shielding.

### 3. Temperature Measurement

The temperature of the block on which the specimens were mounted was determined by means of a platinum resistance thermometer soldered into a hole in the block with Woods metal. The thermometer was calibrated by the National Bureau of Standards between 10°K and 500°C. Temperatures below 10°K were

accurate to only  $\pm 0.1^\circ\text{K}$ . Between 10 and 15°K the block temperature error was  $\pm 0.04^\circ\text{K}$ . From 15 to 20°K the error was  $\pm 0.03^\circ\text{K}$ , between 20 and 25°K it was  $\pm 0.01^\circ\text{K}$ , and above 25°K the block temperature error was negligible.

Temperature differences between the block and each foil were measured by means of a copper-constantan thermocouple between the block and the middle of the foil. The block junctions of the thermocouples were made by soldering three short lengths of constantan wire and a common copper reference wire into a hole in the block directly below the platinum resistance thermometer as indicated in Fig. 1. The foil junctions were made by soldering a piece of copper thermocouple wire to the free end of each constantan wire. To permit shielding the foil junction from irradiation, the junction was not soldered to the foil but rather a small tip of the copper thermocouple wire extending past the junction was soldered to the middle of the foil as shown in Fig. 1. The entire length of the thermocouple wire was shielded so no change of calibration could occur due to irradiation. The three copper thermocouple leads from the foils and the reference thermocouple wire were led outside the cryostat to the thermocouple measuring circuit.

The constantan used was No. 30 Leeds and Northrup thermocouple wire (1938 calibration). The copper was No. 30 Leeds and Northrup thermocouple wire (1921 or 1938 calibration), drawn to 0.004-in. diameter and annealed in a high-vacuum furnace. Leeds and Northrup thermal-free solder was used for all thermocouple junctions.

Thermocouple emf were read with a Rubicon thermofree potentiometer using a high-sensitivity (0.05 microvolt/mm) galvanometer. The emf  $E$  was expressed in the following manner:

$$E = \alpha + \beta \Delta T, \quad (1)$$

where  $\alpha$  was the emf when both junctions of the thermocouple were at the same temperature,  $\beta$  was the thermoelectric power, and  $\Delta T$  was the temperature difference between the block and the foil.  $E$  could be read to  $\pm 5 \times 10^{-8}$  volt.

To determine  $\alpha$  for each of the thermocouples, the three copper thermocouple leads, before being soldered to the constantan wires, were soldered into the hole in the block with the reference wire, and their emf's relative to this reference wire were measured from 5 to 78°K. The voltage  $\alpha$  arose primarily from imperfect cancellation of the Thomson emf's in each pair of copper leads and was therefore sensitive to the distribution of composition inhomogeneities and thermal gradients along the wires. Once the wires were installed in the cryostat, they were not disturbed other than to permit soldering of the junctions. Hence, thermal gradients and inhomogeneities were identical during both the  $\alpha$  determination and the annealing measurements. A check was made on the constancy of  $\alpha$  by making two

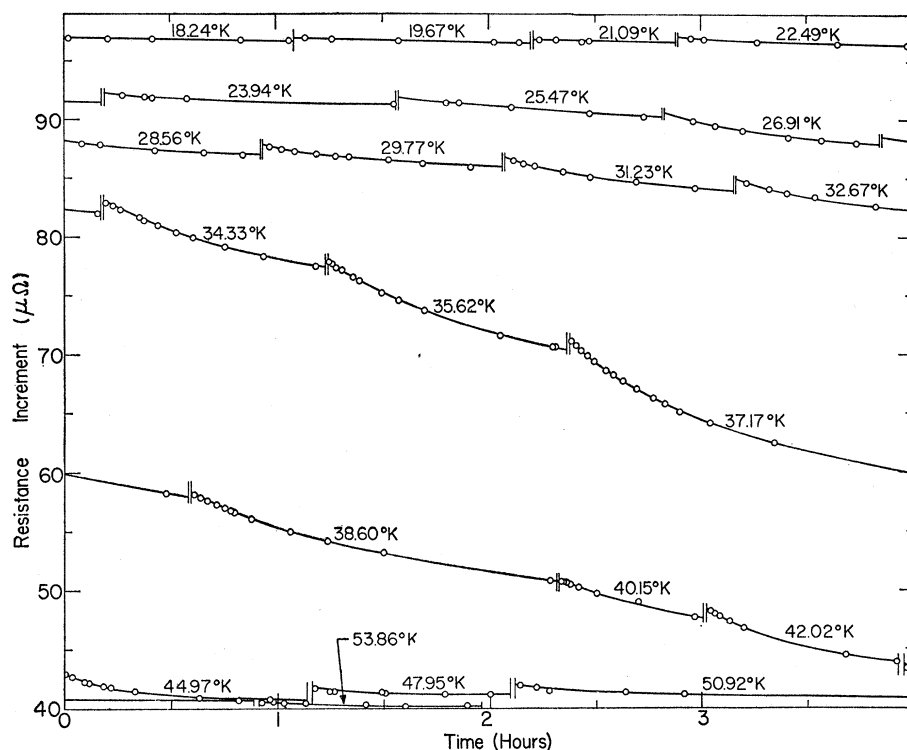


FIG. 2. Isothermal annealing curves between 18 and 54°K of the resistance increment in 99.999% pure Cu.

separate measuring runs. It was found to be reproducible within the experimental error of  $\pm 1 \times 10^{-8}$  volt.

After  $\alpha$  was determined, the three copper thermocouple wires were unsoldered from the block and the foil junctions made as described above. Evidence that additional contributions to  $\alpha$  arising from individual variations in the Peltier emf generated at the junctions were negligible was provided by tests conducted at room temperature on a number of thermocouples between whose junctions small but identical temperature differences were maintained. The emf's produced by these thermocouples agreed to within  $1 \times 10^{-8}$  volt, indicating that variations in all sources of emf in the thermocouple circuits were within this range. Since the thermocouples were at room temperature, Thomson emf's were small and their variations could be disregarded. The tests thus showed that variations in Peltier emf's from one junction to another were within  $1 \times 10^{-8}$  volt at room temperature and, since the Peltier emf decreases with decreasing temperature, less than this at lower temperatures.

An average value of  $\beta$  was obtained from the  $\beta$  values of a number of Cu-constantan thermocouples calibrated in this laboratory.<sup>14</sup> The  $\beta$  values of these thermocouples showed less than 5% variation, and since temperature differences between the block and foils were quite small (less than 3°K for both the Cu and Ag foils), the average value could be used with sufficient accuracy. The maximum error in foil tempera-

ture, including all the above mentioned sources of error, are tabulated in Table I.

Table I also lists the probable error in the temperature intervals between successive anneals. The values take into account the fact that errors arising from variations in  $\beta$  tend to cancel, since the error in  $\beta$  at one temperature will be very nearly equal to the error in  $\beta$  at the next higher temperature.

### III. EXPERIMENTAL RESULTS

Because of improper functioning of the current integrator, only a rough estimate of the total bombardment can be given. However, a careful record was kept of the target box beam current during bombardment. From the total integrated target box beam current and the ratio of total target box beam current to integrated flux,<sup>15</sup> one can calculate the total flux delivered to the foils. The total flux obtained in this manner for this

TABLE I. Temperature errors in various temperature regions.

T (°K)	Maximum error in foil temperature (°K)			Probable error in temperature intervals (°K) Cu and Ag
	Cu	Ag	CuNi	
10-15	$\pm 0.15$	$\pm 0.12$	$\pm 0.15$	$\pm 0.06$
15-20	0.07	0.07	0.10	0.05
20-25	0.05	0.06	0.05	0.03
25-30	0.02	0.02	0.03	0.01
above 30	0.01	0.01	0.01	0.01

<sup>14</sup> R. W. Vook (to be published).

<sup>15</sup> Supplied by R. O. Simmons from the lattice parameter experiment (see reference 6).

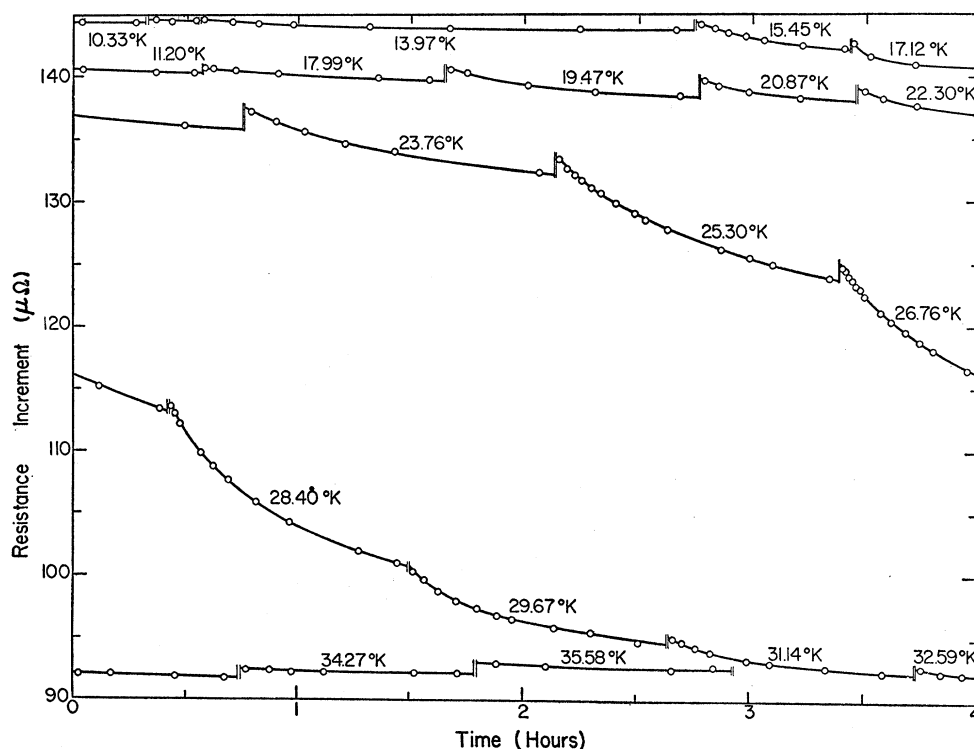


FIG. 3. Isothermal annealing curves between 10 and 35°K of the resistance increment in 99.999% pure Ag.

experiment was  $(2.5 \pm 0.3) \times 10^{16}$  deuterons/cm<sup>2</sup>. Because of the uncertainties in the method it was felt that resistivity increment *versus* flux curves should not be given. The total resistivity increments of the Cu, Ag, and CuNi foils were  $5.61 \times 10^{-8}$  ohm-cm,  $6.87 \times 10^{-8}$  ohm-cm, and  $10.1 \times 10^{-8}$  ohm-cm, respectively.

The isothermal annealing behavior of the resistivity increments due to bombardment in the Cu and Ag foils are shown in Figs. 2 and 3. These curves were obtained by subtracting from the resistance of the foil after bombardment the resistance of the foil before bombardment at the same temperature and converting this increment to a difference in resistivity. To convert resistance to resistivity, the geometrical factor  $A/L$  was determined from the ratio  $\rho_0/R_0$  for each of the three foils, where  $\rho_0$  is the handbook<sup>16</sup> value of the resistivity at 0°C and  $R_0$  is the measured resistance of the foil at the same temperature.

Because of uncertainties regarding the relative lengths of the bombarded and unbombarded sections of the foil, an appreciable systematic error was introduced when the observed resistance change was converted to a resistivity increment. This error amounted to about  $\pm 3.5\%$ . It is believed that effects due to temperature gradients in the Cu and Ag foils were negligible because of the high thermal conductivity of the metals.

The small discontinuities between successive curves represent a change in the thermal contribution to the

resistivity and indicate that an alteration in the lattice vibration spectrum has occurred as a consequence of irradiation.

Figure 4 illustrates the manner in which the resistivity increment in the CuNi foil annealed. For comparison, the annealing behavior of pure Cu and Ag is also shown. The low-temperature annealing has been broadened by the addition of 3.78 atomic % Ni but still appears to be centered about the same temperature, 37°K. No annealing occurs in the Cu between the low-temperature drop and 78°K, whereas a small amount of annealing occurs in the Ag between the low-temperature recovery and 78°K.

Meissner,<sup>17</sup> deHaas *et al.*,<sup>18</sup> and Grüneisen<sup>19</sup> have published resistance *versus* temperature data of various

TABLE II. Resistance *versus* temperature for Cu.  $R_0$  = resistance at 0°C = 5252  $\mu$ ohm.

$T$ (°K)	$10^8 \times (R_T/R_0)$	$T$ (°K)	$10^8 \times (R_T/R_0)$	$T$ (°K)	$10^8 \times (R_T/R_0)$
7.68	0.93	23.46	2.01	43.02	18.73
9.72	0.94	26.40	2.85	45.98	24.19
11.31	0.95	30.26	4.64	49.93	32.84
13.17	0.99	33.18	6.66	54.95	45.86
16.16	1.09	36.10	9.32	59.88	60.89
18.67	1.28	40.02	14.12	76.93	124.68
20.59	1.49				

<sup>17</sup> W. Meissner, *Z. Physik* **38**, 647 (1926) and *Handbuch der Experimental Physik*, edited by W. Wien and F. Harms (Akademische Verlagsgesellschaft, Leipzig, 1935), Vol. 11, Part 2, p. 32.

<sup>18</sup> deHaas, de Boer, and van den Berg, *Physica* **1**, 1115 (1933-1934); W. J. deHaas and G. J. van den Berg, *Physica* **3**, 440 (1936).

<sup>19</sup> E. Grüneisen, *Ann. Physik* **16**, 530 (1933).

<sup>16</sup> For the CuNi foil  $\rho_0$  was obtained from J. O. Linde, *Ann. Physik* **15**, 219 (1932).

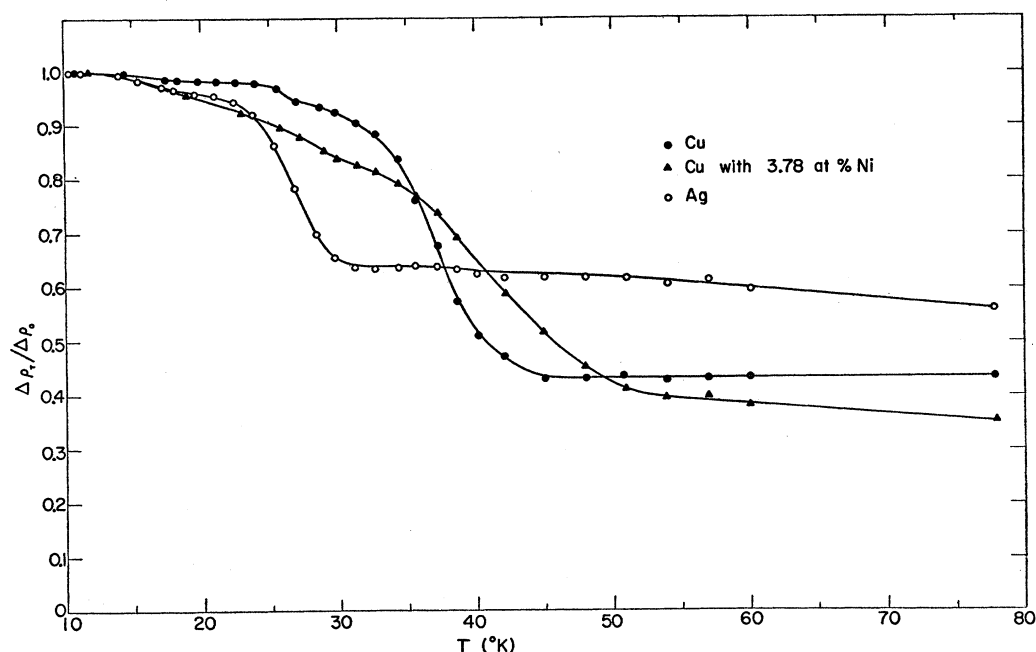


FIG. 4. Annealing behavior of the resistance increment in the three metal foils used in this research. Resistance measurements were made at annealing temperatures. All three foils were held at each temperature for approximately one hour.

pure metals. However, the data are not very detailed between 20 and 60°K, and in some cases the purity was less than that of the metals used in this research. For this reason the resistance *versus* temperature data obtained in this investigation have been tabulated in Tables II-IV.

The Au data in Table IV were obtained in a preliminary cyclotron run which was unsuccessful in obtaining isothermal annealing data but in which annealing of the resistivity increment was observed upon gradual warm up of the specimen. The annealing

TABLE III. Resistance *versus* temperature for Ag.  $R_0$ =resistance at 0°C=6225  $\mu$ ohm.

$T$ (°K)	$10^2 \times (R_T/R_0)$	$T$ (°K)	$10^2 \times (R_T/R_0)$	$T$ (°K)	$10^2 \times (R_T/R_0)$
7.10	0.129	23.29	0.571	43.02	4.706
9.20	0.136	26.27	0.870	45.99	5.720
10.90	0.142	30.17	1.436	49.97	7.176
12.89	0.159	33.09	1.999	55.00	9.145
15.88	0.207	36.05	2.683	59.97	11.196
18.37	0.284	40.00	3.769	77.02	18.582
20.39	0.374				

TABLE IV. Resistance *versus* temperature for Au.  $R_0$ =resistance at 0°C=5134  $\mu$ ohm.

$T$ (°K)	$10^2 \times (R_T/R_0)$	$T$ (°K)	$10^2 \times (R_T/R_0)$	$T$ (°K)	$10^2 \times (R_T/R_0)$
6.76	0.133	26.84	1.799	42.62	6.976
9.91	0.146	32.55	3.381	45.66	8.218
12.78	0.195	33.14	3.564	50.28	10.101
15.99	0.336	37.26	4.957	60.31	14.360
20.65	0.739	38.02	5.225	77.63	21.772
23.40	1.141	40.09	6.002		

was similar to that observed by Cooper.<sup>3</sup> The increment was constant to about 39°K and above this temperature showed a small decrease with each increase in temperature.

The energy of the deuterons striking the foils was about 10.7 Mev, since about 1.3 Mev was lost in traversing the duralumin diaphragm and the two 0.0005-in. copper windows in the thermal radiation shields.

#### IV. DISCUSSION

##### 1. Determination of the Initial Activation Energy Spectra

The existence of thermally activated annealing processes in metals subjected to radiation damage at low temperatures suggests the suitability of assigning to each portion of an observed property change  $P$  a characteristic activation energy  $E$  which governs its recovery rate through the Boltzmann factor  $e^{-E/kT}$ . Thus, if the magnitude of this portion of the property change is denoted by  $p$ , its recovery rate is

$$dp/dt = -Ke^{-E/\tau}, \quad (2)$$

where  $\tau = kT$ . Interpretation of the quantity  $K$  requires specific suppositions regarding the mechanism of recovery. If recovery is assumed to arise from the motion of defects by a series of thermally induced jumps to traps or annihilation centers at which their contribution to the property is reduced,  $K$  will be given by

$$K = fqA/a = pA/a, \quad (3)$$

where  $q$  is the concentration of defects with activation

energy  $E$ ,  $f$  is the contribution to the property change associated with a unit concentration of free defects relative to that associated with the same concentration of trapped or annihilated defects,  $A$  is an appropriate vibration frequency, and  $a$  is the average number of jumps required for the moving defects to reach annihilation centers. For coordinated centers such as would exist if the recovery process were the annihilation of close Frenkel pairs,  $a$  will be a small number of the order of unity. If the defects diffuse to dislocations,  $a$  will be a large number. If the defects diffuse and form new defects by combination, then two cases may arise. First, if the defects which move with a given activation energy can combine only with defects of the same energy, then  $a$  is of the order  $q^{-(n-1)}$ , where  $n$  is the number of defects which combine to form the new defect. Second, if the diffusing defect can combine with defects with other activation energies, then  $a$  is given by the reciprocal of the existing concentration of these defects. The second case is probably more likely to occur in practice. These mechanisms will be referred to as higher order processes of the first and second kinds.

For a sufficiently dense or continuous distribution of activation energies, it is possible to represent the total property change  $P$  by a "spectrum" of processes  $p(E)$  such that

$$P = \int_0^{\infty} p(E) dE. \quad (4)$$

If the value of  $p(E)$  before any annealing has occurred is  $p_0(E)$ , the original value of  $P$  before annealing will be given by

$$P_0 = \int_0^{\infty} p_0(E) dE, \quad (5)$$

and  $p_0(E)$  will be said to constitute an initial activation energy spectrum. The first detailed treatment of the annealing of such continuously distributed processes was given by Primak.<sup>20</sup>

The following remarks will propose a method whereby the approximate shape of  $p_0(E)$  may be determined from the behavior of  $P$  observed during a series of isothermal anneals. It will be assumed that the processes involved are of identical nature (i.e., that the frequency factor  $A$  and the mechanism of recovery are the same for all processes) and differ only in their activation energies.

#### a. Determination of Energies

Because of the exponential dependence of the annealing rate upon the activation energy, processes distributed in activation energy but otherwise identical anneal in order of increasing energy, the energy range of processes undergoing simultaneous annealing at a

measurable rate being of the order of a few  $kT$ . For density functions  $p_0(E)$  appreciably broader than this, the annealing of a process with any given activation energy is not accompanied by a significant change in the magnitude of the observed property and hence in the damaged state of the metal. Thus, even with a diffusive mechanism, the value of  $a$  in Eq. (3) will remain, as for a monomolecular mechanism, essentially constant throughout the annealing of such a process, and integration of Eq. (2) shows that

$$p(E) = p_0(E) \exp\left(\frac{-At}{a(E)} e^{-E/\tau}\right), \quad (6)$$

where  $a(E)$  is an appropriate value of  $a$  for the particular process.<sup>21</sup> After a succession of anneals at various temperatures,  $p$  is given by

$$p = p_0 \exp\left[-\frac{A}{a(E)} (t_1 e^{-E/\tau_1} + t_2 e^{-E/\tau_2} + \dots + t_n e^{-E/\tau_n})\right] \\ = p_0 \theta(E). \quad (7)$$

It will be useful to consider the factor  $\theta$  as a function of  $E$ . This is plotted in Fig. 5.<sup>20</sup> Although the precise shape of the curve will depend upon the annealing history and upon the manner in which the quantity  $a(E)$  varies with energy, it will usually show the general features of the curve illustrated—an abrupt rise in  $\theta$  from 0 to 1 within a small energy range of the order of  $2kT$  in extent. As time progresses at a given temperature, the curve will move to the right with decreasing rate and with essentially unaltered form.

From Eq. (7), the activation energy corresponding to a given value of  $\theta$  is

$$E_\theta = \tau_n \left\{ \ln\left(\frac{-A/a(E)}{\ln\theta}\right) + \ln\left[ t_1 \exp\left(-E_\theta\left(\frac{1}{\tau_1} - \frac{1}{\tau_n}\right)\right) \right. \right. \\ \left. \left. + \dots + t_{n-1} \exp\left(-E_\theta\left(\frac{1}{\tau_{n-1}} - \frac{1}{\tau_n}\right)\right) + t_n \right] \right\}. \quad (8)$$

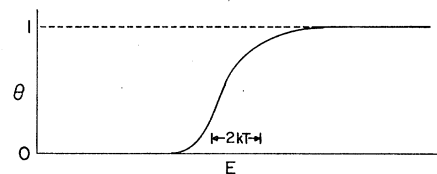


FIG. 5. The annealing function  $\theta$ .

<sup>21</sup> The case of a continuum of higher order processes of the first kind has been treated by Primak. However, it is difficult to imagine a recovery mechanism which would require the postulation of such a continuum or, if the distribution were genuinely continuous, how annealing could proceed at a measurable rate. Under such circumstances  $a$  will be of the order of  $(p(E)dE/f)^{1-n}$  and will be large without limit since  $p(E)dE$  is infinitesimal. The exponent in Eq. (6) will then be zero and  $p/p_0$  will have the constant value of one.

<sup>20</sup> W. Primak, Phys. Rev. **100**, 1677 (1955).

The approximate energy of the actively annealing processes (i.e., that energy for which  $\theta$  has a value near one-half) at the end of an anneal can be found by the formula<sup>22</sup>

$$E = \frac{\tau_{n+1}\tau_n}{\tau_{n+1} - \tau_n} \ln R, \quad (9)$$

where  $R$  is the ratio of the annealing rate at the beginning of the  $(n+1)$ th anneal to that at the end of the  $n$ th anneal. The value of  $\ln[-A/a(E) \ln \theta]$  can then be calculated and a good estimate of this quantity obtained from the average of a number of such determinations. Since  $A$  will be a large number (of the order of  $10^{13}$ ), the value thus found will be applicable to all energy regions in which  $a(E)$  does not differ by a large factor from its value in the region where the determination was made. This will in general include quite a wide range of energies. Once the determination is made, the energy corresponding to an intermediate value of  $\theta$  may be calculated by Eq. (8) for any point in the annealing history, even in temperature regions where good annealing rate measurements cannot be made. The second term in the bracket will not be highly sensitive to values of  $E_\theta$ , and, if

$$t_n \gg t_{n-1} \exp\left[-E_\theta \left(\frac{1}{\tau_{n-1}} - \frac{1}{\tau_n}\right)\right], \quad (10)$$

sufficiently accurate values of the energies may be obtained by using estimated values of  $E_\theta$  in the exponents. In the application to deuteron-irradiated specimens in this investigation,  $t_n$  was more than five times larger than the preceding term.

Considering a constant value of  $\theta=C$ , the change in the energy value associated with the same degree of completion of the annealing process occurring between two points  $A$  and  $B$  in the annealing history is given by

$$\begin{aligned} \Delta E_C^{AB} = & (\tau_B - \tau_A) \left[ \ln \left( \frac{-A/\bar{a}(E)}{\ln C} \right) \right] \\ & + \tau_B \ln \left\{ t_1 \exp \left[ -E_C^B \left( \frac{1}{\tau_1} - \frac{1}{\tau_B} \right) \right] + \dots \right. \\ & \left. + t_A \exp \left[ -E_C^B \left( \frac{1}{\tau_A} - \frac{1}{\tau_B} \right) \right] + \dots + t_B \right\} \\ & - \tau_A \ln \left\{ t_1 \exp \left[ -E_C^A \left( \frac{1}{\tau_1} - \frac{1}{\tau_A} \right) \right] + \dots + t_A \right\}, \end{aligned} \quad (11)$$

where  $\bar{a}(E)$  is a suitable intermediate value of  $a(E)$  for the interval. If the value of  $a(E)$  is assumed not to vary by a large fraction over the interval, the value

found for  $\ln\{-A/[a(E) \ln C]\}$  may be used in the calculation of  $\Delta E_C$ .

#### b. Determination of $p_0$

At any stage in the annealing process the annealing function  $\theta$  may be replaced by a step function positioned at an energy  $E'$  such that

$$P = \int_0^\infty p(E) dE = \int_{E'}^\infty p_0(E) dE. \quad (12)$$

The value of  $E'$ , like the value of  $E_C$ , will assume higher values as annealing progresses. Between two points in the annealing process, the change in the property value  $P$  will be

$$\Delta P = p_0(\bar{E}') \Delta E', \quad (13)$$

where  $\bar{E}'$  is a suitable intermediate value of  $E'$  for the interval. Dividing by the value of  $\Delta E_C$  for the same interval and solving for  $p_0(\bar{E}')$ , one obtains

$$p_0(\bar{E}') = \frac{\Delta P}{\Delta E_C} \frac{\Delta E_C}{\Delta E'}. \quad (14)$$

The value of  $\theta(E')$  will depend upon the value of  $dp_0(E)/dE$ , being larger for greater values of  $dp_0(E)/dE$ . In an energy region where  $dp_0(E)/dE$  is increasing, therefore, values of  $\Delta E'$  will exceed those of  $\Delta E_C$  and  $\Delta E_C/\Delta E'$  will be less than one. Similarly, in regions of decreasing  $dp_0(E)/dE$ ,  $\Delta E_C/\Delta E'$  will be greater than one. For a rather slowly varying distribution function  $p_0(E)$ ,  $\theta(E')$  will have a value near one half and will remain essentially constant as annealing progresses. Thus  $\Delta E_C/\Delta E'$  will be near unity<sup>23</sup> and one may write

$$p_0(\bar{E}') \cong \Delta P / \Delta E_C. \quad (15)$$

Since the values of  $E_C$  obtained from Eq. (8) relate to partially annealed processes and are thus very near the corresponding values of  $E'$ , for sufficiently small annealing intervals we may associate the values of  $p_0(\bar{E}')$  found from Eq. (14) with the arithmetical average of  $E_C$  found from Eq. (8) for the extremities of the interval.

The process outlined above may be repeated for many successive intervals to yield a set of points  $p_0(E)$  which will characterize the spectrum of recovery processes. The results will not be entirely accurate, since in most actual circumstances the conditions imposed upon  $p_0(E)$  and  $a(E)$  will be only partially satisfied. They can nevertheless provide information regarding the approximate intensity and energy distribution of important recovery processes and also a value of the ratio of the frequency factor to the average number of jumps.

The initial activation energy spectra for the annealing of resistivity increments that result from applying the

<sup>23</sup> For the spectra investigated in this research  $1.1 > \Delta E_C / \Delta E' > 0.9$ .

<sup>22</sup> A. W. Overhauser, Phys. Rev. **90**, 393 (1953).



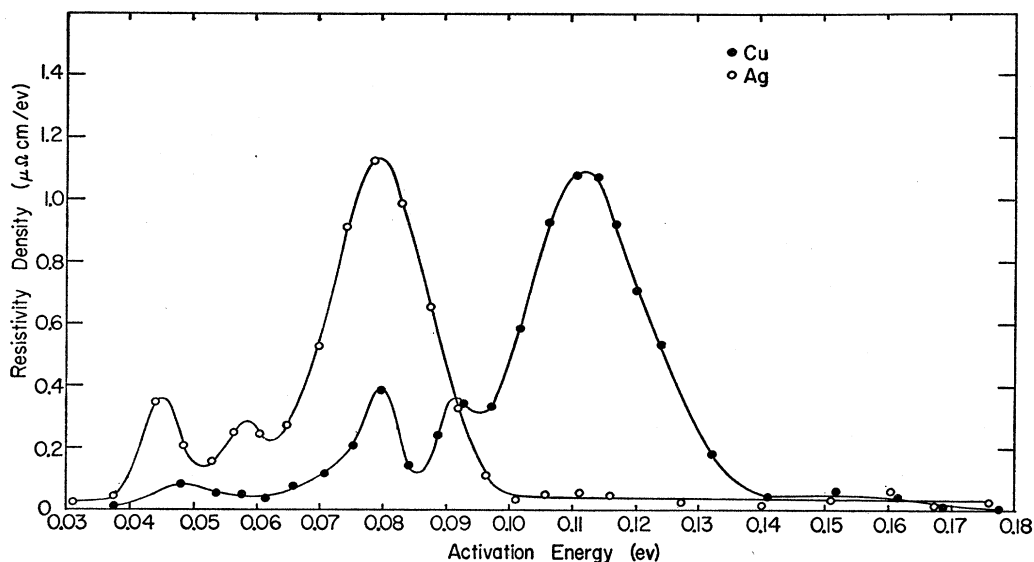


FIG. 6. The initial activation energy spectra for the annealing of resistivity increments in pure Cu and Ag.

above analysis to the isothermal annealing data obtained in this research are shown in Fig. 6. The contribution to the resistivity increment due to the change in the lattice vibration spectrum has been subtracted out, as explained in Sec. 2 below, so that Fig. 6 represents the resistivity-distribution due to defects only. The value of  $\ln(A/a)$  was  $27 \pm 2$  for both metals.

## 2. Change in the Debye Characteristic Temperature

The discontinuities between successive isothermal annealing curves indicate a change in the lattice vibration spectrum which can be most easily represented as a change in the resistive Debye characteristic temperature of the metal. After bombardment the thermal part of the resistivity of the foils at any temperature  $T$  (low enough so little annealing has occurred) can be obtained by adding to the thermal part of the resistivity of the foils before bombardment the sum of the discontinuities up to that temperature. The thermal part of the resistivity of metals  $\rho_T$  is usually represented by the Bloch Grüneisen formula<sup>24</sup> as follows:

$$\rho_T = \frac{K T^5}{M \Theta^6} \int_0^{\Theta/T} \frac{z^5 dz}{(e^z - 1)(1 - e^{-z})}, \quad (16)$$

where  $M$  = atomic weight,  $\Theta$  is the Debye characteristic temperature, and  $K$  is a constant characteristic of the metal and its volume.

Assuming that Eq. (16) is valid, one obtains, on multiplying both sides by  $T$ ,

$$\rho_T T = \frac{K}{M} \left(\frac{T}{\Theta}\right)^6 \int_0^{\Theta/T} \frac{z^5 dz}{(e^z - 1)(1 - e^{-z})}. \quad (17)$$

Since  $\rho_T T$  is a function of  $T/\Theta$  only, a plot of  $\rho_T T$  versus  $T$  for the foils before and after bombardment will be of identical form but will suffer a change of scale because of the difference in the Debye characteristic temperatures. Let  $\Theta_1$  be the Debye characteristic temperature of the foil before bombardment and  $\Theta_2$  that of the foil after bombardment. Thus, for any fixed value of  $\rho_T T$ , one has the simple relation

$$T_1/\Theta_1 = T_2/\Theta_2 \quad (18)$$

at temperatures low enough so little annealing has occurred.

If  $\Theta_2$  is written as  $\Theta_2 = \Theta_1 + \Delta\Theta$ , one obtains

$$\Delta\Theta = \Theta_1 \left( \frac{T_2 - T_1}{T_1} \right). \quad (19)$$

Since  $T_2$  is less than  $T_1$  (i.e., the thermal part of the resistivity of the foil after bombardment increases more rapidly with temperature than that of the original metal),  $\Delta\Theta$  is negative.

For Cu, the  $\Delta\Theta$  calculated in this manner was  $-(15 \pm 1^\circ\text{K})$ , assuming  $\Theta_1 = 333^\circ\text{K}$  and using values of  $\rho_T T$  below  $25^\circ\text{K}$ . For Ag,  $\Delta\Theta$  was  $-(10 \pm 1^\circ\text{K})$ , assuming  $\Theta_1 = 223^\circ\text{K}$  and using values of  $\rho_T T$  below  $15^\circ\text{K}$ . The  $\Delta\Theta$  in Cu is comparable to that found by Bowen and Rodeback.<sup>25</sup> These authors plot  $\Delta\Theta$  as a function of residual resistivity of Cu irradiated at liquid nitrogen temperatures with 33.6-Mev  $\alpha$  particles. For a residual resistivity equal to that of the bombarded Cu in the present research, they obtained a  $\Delta\Theta$  of about  $-21^\circ\text{K}$ .

<sup>24</sup> D. K. C. MacDonald, *Handbuch der Physik* (Springer-Verlag, Berlin, 1956), Vol. 14, p. 137.

<sup>25</sup> D. Bowen and G. W. Rodeback, *Acta Met.* **1**, 649 (1953).

An estimate of the annealing of the  $\Delta\Theta$  can be obtained from the behavior of the discontinuities. Let  $\Delta$  represent the discontinuity when the temperature was increased by  $\Delta T = T_2 - T_1$ ; it can therefore be expressed in the following manner:

$$\Delta = [\rho_T(T_2, \Theta_2) - \rho_T(T_1, \Theta_2)] - [\rho_T(T_2, \Theta_1) - \rho_T(T_1, \Theta_1)]. \quad (20)$$

Equation (20) can be written as

$$\begin{aligned} \Delta &= \left[ \left( \frac{\partial \rho_T}{\partial T} \right)_{\Theta_2} - \left( \frac{\partial \rho_T}{\partial T} \right)_{\Theta_1} \right]_{\bar{T}} \Delta T \\ &= \left[ \frac{\partial}{\partial \Theta} \left( \frac{\partial \rho_T}{\partial T} \right) \right]_{\bar{T}, \bar{\Theta}} \Delta T \Delta \Theta \\ &= \left[ \frac{-1}{\Theta^3} \frac{d^2(\rho_T T)}{d(T/\Theta)^2} \right]_{\bar{T}, \bar{\Theta}} \Delta T \Delta \Theta, \quad (21) \end{aligned}$$

where  $\bar{T}$  and  $\bar{\Theta}$  are suitable intermediate values of  $T$  and  $\Theta$ . One thus obtains the following expression for  $\Delta\Theta$ :

$$\Delta\Theta = -\Theta^3 \frac{\Delta/\Delta T}{[d^2(\rho_T T)/d(T/\Theta)^2]}. \quad (22)$$

The  $\Delta\Theta$  versus temperature curves shown in Fig. 7 were obtained using Eq. (22). The large scatter is due to scatter in the  $\Delta/\Delta T$  values, so high accuracy is not claimed. The second derivative term was found using the Bloch-Grüneisen formula. In finding the second derivative of  $\rho_T T$  for Ag, allowance was made for the deviation of Ag from the Bloch-Grüneisen formula described by variation in the Debye characteristic temperature with temperature.<sup>26</sup>

The resistance that anneals out during any one isothermal anneal includes a contribution due to the annealing of the change in the Debye characteristic

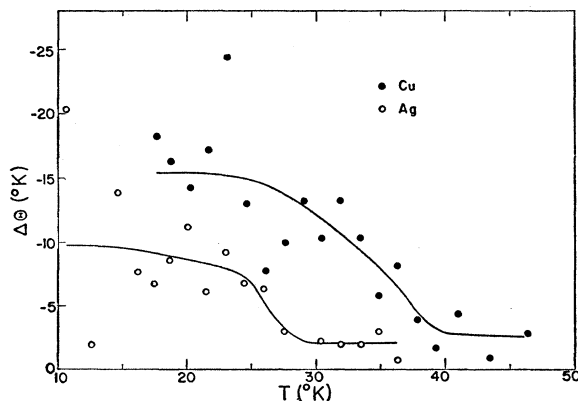


FIG. 7. Annealing of the radiation-induced decrease in the Debye characteristic temperature.

<sup>26</sup> F. M. Kelly, Can. J. Phys. 32, 81 (1954).

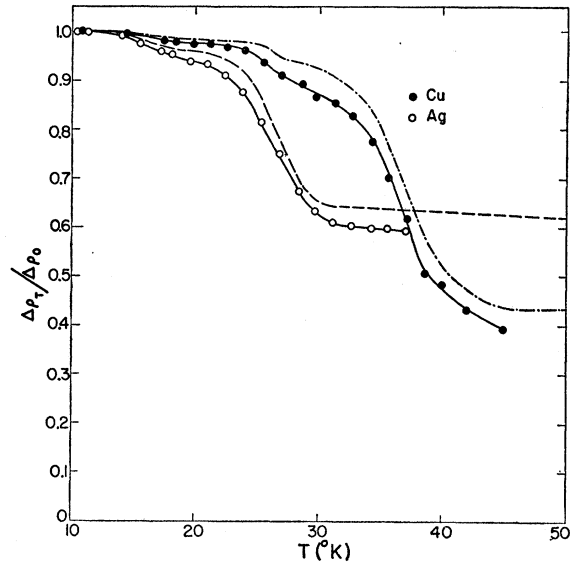


FIG. 8. Annealing behavior of the resistance increment in the Cu and Ag foils corrected for the decrease in the Debye characteristic temperature. The uncorrected Cu and Ag curves of Fig. 4 are shown dashed for comparison.

temperature. An estimate of this contribution can be obtained from the expression

$$\frac{\partial \rho_T}{\partial \Theta} = -\frac{1}{\Theta^2} \frac{d(\rho_T T)}{d(T/\Theta)}. \quad (23)$$

Thus, if an amount  $\delta(\Delta\Theta)$  of the decrease in the Debye characteristic temperature anneals out, the resulting resistivity change is

$$\delta(\Delta\Theta) \frac{\partial \rho_T}{\partial \Theta} = -\frac{\delta(\Delta\Theta)}{\Theta^2} \frac{d(\rho_T T)}{d(T/\Theta)}. \quad (24)$$

From the  $\Delta\Theta$  annealing curves in Fig. 7, the contribution given by Eq. (24) was calculated and subtracted from the resistivity annealed out in each isothermal anneal. The resistivity densities in Fig. 6 result therefore from changes in defect concentration only, excluding the effect of the defects on the Debye characteristic temperature. This effect was greatest, of course, where  $\Delta\Theta$  was annealing most rapidly and amounted to about a 10% reduction in height of the large peaks in the activation energy spectra.

Similarly, the resistance increments in Cu and Ag indicated in Fig. 4, determined by comparing bombarded and unbombarded resistance values at the annealing temperature, are too large since the decrease in the Debye characteristic temperature results in an increase in the thermal part of the resistance of the foils after bombardment. Figure 8 was drawn taking this into account and shows the Cu and Ag curves of Fig. 4 dashed for comparison. The curves are drawn only up to the highest temperatures at which  $\Delta\Theta$  was

measured. Note that a larger percentage of the damage anneals out than is indicated in Fig. 4.

### 3. Summary

The major experimental results found in this experiment are as follows:

(1) The annealing spectrum in very pure noble metals is simple. In the 15°K to 80°K range it consists of a number of small peaks followed by a large peak. These peaks in the activation energy spectrum are reasonably discrete. If one assumes that several point defects are produced per primary and that the separation distances of these defects are of the order of two to ten or twenty lattice parameters, then it is not too surprising to find some spread in the activation energies, especially since the spread is only of order 0.01 ev.

(2) The frequency factor ( $A/a$ ) is large, having a value in the range between  $7.2 \times 10^{10}$  and  $3.9 \times 10^{12}$  for both copper and silver.

(3) The Debye characteristic temperature decreases on irradiation. For copper the decrease after  $2.5 \times 10^{16}$  deuterons per  $\text{cm}^2$  was 15°K, for silver the decrease was 10°K. Most of this change anneals out on warming to 50°K.

(4) Alloying tends to make the annealing more nearly a continuous process with a wide range of activation energies.

(5) No large low-temperature drop in resistivity was found for pure gold in the range 12 to 50°K.

### V. INTERPRETATION

The following models have been proposed to explain the low-temperature annealing of irradiated noble metals:

(a) Close pairs with interstitials mobile at about 30°K.

(b) Close pairs with interstitials mobile at about 190°K.

(c) Movement of interstitials as crowdions.

(d) Interstitials changing character, i.e., point interstitials changing to crowdions.

(e) A trapping of interstitials by interstitials as a result of the anisotropic interaction potential between point defects.

The structure involved in the low-temperature annealing points strongly towards close pairs. It should be noted that this does not necessarily mean that interstitials have cubic rather than uniaxial symmetry. Tewordt<sup>27</sup> has calculated the energies required to make a point interstitial and a crowdion (i.e., a uniaxial interstitial) in copper. He finds that the energy to make a point interstitial in copper is about 2.55 ev, whereas the energy required to make a crowdion is 3.2 ev. He also calculated the energy required to form a lattice vacancy

in copper. This energy he found to be 0.95 ev. Tewordt<sup>27</sup> has also calculated the volume changes to be expected if one takes an atom from the surface and inserts it into an interstitial position. The volume increase found was 0.84 atomic volume. If a vacancy is created by taking a lattice atom out and placing it on the surface, Tewordt finds that the volume of the solid increases by 0.51 atomic volume in copper.

Let us attempt to use this information first to determine the concentrations of displaced atoms produced during irradiation and second to decide what happens during the prominent annealing process at about 30°K.

During irradiation the concentration of vacancies equals the concentration of interstitials. Now Vook and Wert<sup>5</sup> found that  $\Delta V/V = 1.14 \times 10^{-20}$  per deuteron per  $\text{cm}^2$ . This value applies to an average deuteron energy of 8.5 Mev.

From Tewordt's<sup>27</sup> calculations for the increase in volume, the fraction of atoms displaced per deuteron is related to the volume change as follows:

$$f(\Delta v_i + \Delta v_v) = \Delta V/V, \quad (25)$$

where  $\Delta v_i$  and  $\Delta v_v$  are the volume increases for an interstitial and a vacancy, respectively, measured in atomic volumes. Thus  $f = 0.84 \times 10^{-20}$  per deuteron, so that the fractional defect concentration after  $10^{17}$  deuterons per  $\text{cm}^2$  would be  $0.84 \times 10^{-3}$ .

Cooper, Koehler, and Marx<sup>3</sup> found that the initial slope of their curve of resistivity *versus* integrated flux was such that  $10^{17}$  deuterons per  $\text{cm}^2$  would give a resistivity increase of  $0.23 \times 10^{-6}$  ohm cm. Their average energy was near 9.5 Mev. Correcting their average energy to that of Vook and Wert and assuming that the damage is proportional to the reciprocal of the deuteron energy one finds that  $10^{17}$  deuterons per  $\text{cm}^2$  of energy 8.5 Mev would give a  $\Delta\rho = 0.26 \times 10^{-6}$  ohm-cm. Hence the resistivity of 1% of the defects would be  $3.0 \times 10^{-6}$  ohm cm.

Simmons and Balluffi<sup>6</sup> have made lattice parameter measurements during deuteron irradiation at 12°K and during subsequent annealing. They found that the fractional lattice parameter increase was  $4.1 \times 10^{-21}$  per deuteron per  $\text{cm}^2$ . Correcting this for the fact that their deuteron energy was 7 Mev, one finds that  $\Delta d/d = 3.4 \times 10^{-21}$  per deuteron per  $\text{cm}^2$  for 8.5-Mev deuterons. If the lattice expands isotropically, this corresponds to a  $\Delta V/V = 3\Delta d/d = 1.02 \times 10^{-20}$  per deuteron per  $\text{cm}^2$ , which agrees well with Vook and Wert.

Let us next examine the changes which occur upon annealing to 60°K. The most obvious assumption is to suppose that interstitials combine with vacancies. Then  $\Delta f_i = \Delta f_v$ , and the same fractional drops would take place in resistivity, volume, and lattice parameter, since the annealing would simply wipe out a certain fraction of the damage without altering the ratio of the number of vacancies to interstitials. The cyclotron data certainly support this hypothesis, since 37% of the defect resistivity is left, 37% of the lattice parameter

<sup>27</sup> L. Tewordt, Phys. Rev. **109**, 61 (1958).

change is left, and 36% of the volume change still remains at 60°K.

There are two problems which one encounters if this explanation is adopted: first, the results are not consistent with the stored energy measurements made by Blewitt, Coltman, Noggle, and Homes.<sup>7</sup> They irradiated copper in the Oak Ridge pile at 21.7°K. The integrated fast flux was  $4 \times 10^{17}$  neutrons per cm<sup>2</sup>. The resistivity drop on annealing a companion specimen to 60°K was about  $1.73 \times 10^{-9}$  ohm-cm. Thus  $\Delta f$  was  $0.577 \times 10^{-5}$ . If it takes 3.5 eV =  $1.34 \times 10^{19}$  cal to produce one interstitial vacancy pair, then the expected energy release would have been  $\Delta E = 1.34 \times 10^{-19} \times 6.025 \times 10^{23} \times 0.577 \times 10^{-5} = 0.466$  cal/mole. The Oak Ridge experiments showed a release of energy which was less than 0.2 cal/mole in this region. This disagreement is probably not too serious, since there are minor effects connected with the trapping of interstitials which may remove the discrepancy.

Second, why doesn't the damage all anneal out once the interstitials begin to move? It is possible that interstitials trap interstitials as a result of the anisotropic elastic interaction discussed by Eshelby.<sup>28</sup> He showed that for a pair of interstitials in copper,

$$E = 7.5(a_0/r)^3 \Gamma, \quad (26)$$

where

$$\Gamma = l^4 + m^4 + n^4 - \frac{3}{5}. \quad (27)$$

Here  $E$  is the interaction energy in electron volts;  $l$ ,  $m$ ,  $n$  are the direction cosines of the radius vector  $r$  joining the two interstitials, and  $a_0$  is the cube edge. The coordinate axes are taken along the cube axes of the copper crystal. Since  $\Gamma = +0.40$  for a [100] direction the interstitials repel in that orientation, but  $\Gamma = -0.27$  for a [111] direction, and hence the interstitials *attract* in that orientation. Now the interstitials can only move along [100] directions. Consequently two interstitials may trap one another since the possible atomic jumps may lead to an arrangement of higher energy.

Figure 9 shows the various interstitial configurations possible. Keeping one interstitial fixed and calculating

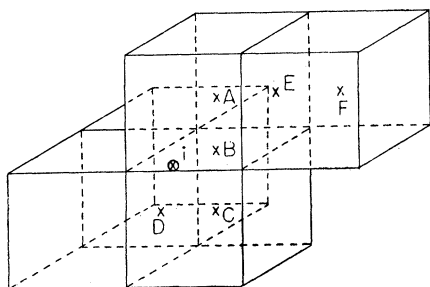


FIG. 9. Possible interstitial configurations.  $\otimes$  denotes the fixed interstitial. Positions  $B$ ,  $D$ , and  $E$  are face center positions. The other positions are at cube centers.

<sup>28</sup> J. D. Eshelby, in *Solid State Physics*, edited by F. Seitz and D. Turnbull (Academic Press, Inc., New York, 1956), Vol. 3, p. 79.

TABLE V. Interaction energy for two interstitials at various positions in copper.

Interstitial position	Interaction energy (ev)	Total energy (ev)
<i>A</i>	-0.144	-0.144
<i>B</i>	-0.161	-0.048
<i>C</i>	-0.100	-0.100
<i>D</i>	+0.162	+0.275
<i>E</i>	-0.068	+0.045
<i>F</i>	-0.019	-0.019

the pair energy using Eq. (26), one obtains the results shown in Table V. Some of the positions shown are saddle point positions, so that the energy of motion (assumed to be unchanged) must be added to the interaction energy to give the total energy of the system. This result is also shown in Table V. From the table it is clear that two interstitials can trap one another in the [111] orientation, since on moving in any [100] direction from position  $A$  the energy increases. Actually, a careful atomic calculation of the interstitial interaction should be made, since we are using Eshelby's equation obtained for an elastic continuum at separations which are a few atomic distances. It is also of interest that this hypothesis provides a simple explanation of the reason why 85% of the resistivity increment anneals out below 80°K in copper after irradiation with 1.35-Mev electrons.<sup>4</sup> In the electron irradiation the number of displacements per primary displaced atom is nearly one, so that a vacancy and an interstitial are produced close together, and in most cases there is no second interstitial present. Hence the above trapping cannot occur for most of the Frenkel pairs.

The frequency factor found in this experiment was in the range between  $7.2 \times 10^{10}$  and  $3.9 \times 10^{12}$ . Actually, it may not be the same for the small peaks as it is for the large peak, but the present accuracy is not good enough to detect a gradual change as one anneals through the activation energy spectrum. The important point is that the frequency factor is large. This shows that the defects which move travel only a short distance. If the atomic vibration frequency is  $10^{13}$ , then the number of atomic jumps made by a defect during an average annealing process is at most  $10^{13}/(7.2 \times 10^{10}) = 139$ . For a random walk process this would correspond in copper to a defect-sink separation distance of about 12 interatomic distances. Note that the actual separation distance could be as small as 2 or 3 interatomic distances if the upper limit for the frequency factor is used. Thus the present data indicate that the defects which anneal at about 30°K travel only a few atomic distances. This is consistent with the general picture that each displaced primary produces a number of displaced atoms all of which remain in a volume within a few atomic distances from their original lattice positions.<sup>29</sup>

<sup>29</sup> See Seitz and Koehler, reference 1.

To summarize, it appears that model (*a*) gives a reasonable explanation for most of the present experimental data. In addition, a trapping model is proposed to explain why all of the damage does not anneal once interstitials begin to move. A measurement of the stored energy released in cyclotron-irradiated specimens during annealing from 15°K to 60°K would be extremely useful.

#### ACKNOWLEDGMENTS

The authors would like to thank many members of the radiation damage group at the University of Illinois for their assistance in making measurements, the cryogenics group under the direction of Professor D. E. Mapother for liberal quantities of liquid helium, and the cyclotron crew under the direction of Professor J. S. Allen for the deuteron bombardments.

## Absolute Energy to Produce an Ion Pair in Various Gases by Beta Particles from $S^{35}$ †

WILLIAM P. JESSE  
*St. Procopius College, Lisle, Illinois*  
 (Received November 21, 1957)

A repetition has been carried out of recent experiments in which the absolute average energy  $W_\beta$  required to form an ion pair in various gases was determined for the beta particles from  $S^{35}$ . The present experiments employ a new procedure, which eliminates almost entirely large correction terms necessary in the former ionization measurements. The two experiments are in good agreement and yield the modified values of 35.0, 24.6, and 33.9 ev/ion pair for  $W_\beta$  for  $N_2$ ,  $C_2H_6$ , and air, respectively.

#### INTRODUCTION

IN a previous paper,<sup>1</sup> henceforth referred to as J and S, results were obtained for  $W_\beta$ , the average energy to produce an ion pair in air, ethylene, ethane, and nitrogen by the beta particles from  $S^{35}$ . Unfortunately, the ionization chamber measurements required corrections of from two to five percent. Although such corrections could apparently be estimated with great precision, they are nevertheless somewhat disturbing. A procedure for eliminating such corrections to a large extent was indicated in J and S, and by this method additional results have been obtained, which are briefly reported here.

In the previous experiments the  $S^{35}$  source was deposited upon a thin plastic film supported upon an annular mount of aluminum. The two principal corrections resulted from a loss of measured ionization when the beta particles struck the wall of the mount, either immediately after their ejection or after being backscattered from the molecules of the gas in the chamber. Both of these cases were discussed in detail in J and S.

It was further pointed out that in measurements with gas at sufficiently high pressure the directly ejected beta particle could be absorbed before reaching the wall, and the backscattered particles, instead of hitting the ring, would pass through the central film with no serious loss in energy. Accordingly the ionization experiments have been repeated with gas pressures high enough to realize to a large extent these conditions.

#### EXPERIMENTAL RESULTS

The technique employed was almost identical with that of J and S. The ionization chamber (Fig. 1) was, however, made smaller and with sturdy metal fittings to withstand a pressure of eight atmospheres. The beta-emitting samples previously measured were mounted at the center of the chamber, supported directly on the collecting electrode post by a thin brass retaining ring.

The technique of making the ionization current measurements was the same as in previous experiments. As before, the ionization currents were always measured successively with the chamber wall at a positive and then at a negative potential with regard to the central electrode and the mean current taken. For these experiments the current difference was insignificant—usually one to two tenths of a percent higher for the positive wall. One might be tempted to attribute this small difference to an acceleration and deceleration of the beta particle in the applied field of the chamber.

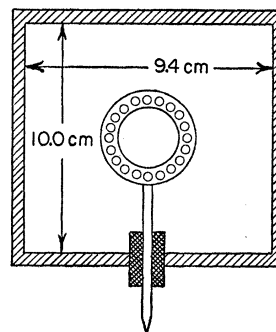


FIG. 1. Schematic diagram of ionization chamber for beta-particle current measurements.

† This work was supported in part by the U. S. Atomic Energy Commission.

<sup>1</sup> W. P. Jesse and J. Sadauskis, Phys. Rev. **107**, 766 (1957).